Investigation of Error in 2D Vibrotactile Position Cues with respect to Visual and Haptic Display Properties: A Radial Expansion Model for Improved Cuing

Nicholas G. Lipari, Christoph W. Borst, and Vijay B. Baiyya

Center for Advanced Computer Studies
University of Louisiana at Lafayette
301 E. Lewis St., Lafayette, LA 70503
{ngl3747,cborst,vbb4359}@cacs.louisiana.edu
http://vrlab.cmix.louisiana.edu

Abstract. We present a human factors experiment aimed at investigating certain systematic errors in locating position cues on a rectangular array of vibrating motors. Such a task is representative of haptic signals providing supplementary information in a collaborative or guided exploration of some dataset. In this context, both the visual size and presence of correct answer reinforcement may be subject to change. Consequently, we considered the effects of these variables on position identification. We also investigated five types of stimulus points based on the stimulus' position relative to adjacent motors. As visual size increases, it initially demonstrates the dominant effect on error magnitude, then correct answer feedback plays a role in larger sizes. Radial error, roughly the radial difference in the stimulus and response position, modeled the systematic error. We applied a quadratic fit and estimated a calibration procedure within a 2-fold cross validation.

Key words: haptics, human factors, user-calibration, collaboration

1 Introduction

An ongoing trend in the interaction and visualization literature is the call for increased availability of multi-sensory feedback. We present an experiment aimed at investigating Subjects' accuracy when locating a haptic stimulus presented at the palm of the hand. This study is a new work to verify a claim made in [1] concerning some systematic errors thought to be present in the experimental results. Specifically, the mean error was near zero at center of the display device, a rectangular array of vibratory motors seen in Figure 1. Error then increased as stimuli moved away from the device's center. A metric we termed radial error

This is an author-formatted version. The original publication is available at www.springerlink.com. ICEIS 2009. Lecture Notes in Business Information Processing, vol 24. pp. 963-974

models the radial expansion that depends on the stimulus' radial distance from device center. The Subjects' responses are then used to create a calibration model of stimulus radius versus radial error.

Two pathways to consider when investigating systematic errors in locating position cues are physiological and psychological. In the former, mechanoreceptors in the palm receiving stimuli and the physical properties of our haptic display device are a concern. For this reason, we choose stimulus points of a sufficient density, given the device's resolution. Psychological operations such as the mental mapping from stimulus, to visual field, to triggering a kinesthetic response are also relevant. Here, the visual display properties of visual size and correct answer reinforcement are of interest.

There have been several recent attempts to commercialize standard input devices with integrated haptic feedback mechanisms. The VTPlayer mouse consists of two finger-pad pin arrays. Marketed toward visually-impaired computer users, recent literature [2] has shown this device to effectively convey basic directional information. In their study, both static and animated indicators were rendered for the Subjects. Other commercial devices with larger markets are Logitech's iFeel Mouse and RumblePad, the Novint Falcon, and Sensable's line of Phantom force-feedback styli.

Several works, e.g. [3, 4, 5, 6], evaluated the effectiveness of haptic devices and the display properties relevant to efficient communication. In [3], tactors stimulated opposing sides of the wrist. The authors estimated an Information Transfer measure of 1.99 bits (almost 4 locations) for both sides combined. The experiment in [6] used a force-feedback pen device. The results suggested that 2.8 levels of stiffness and 2.9 levels of force magnitude can be perceived by Subjects. The authors of [4, 5] examined subject localization ability with regard to the forearm and the abdomen. They found stimulus position relative to body landmarks to be a major factor in localization.

Several studies [7, 8, 9] have investigated tactile stimulus for communication of directional cues. The experiment in [8] extends the "Sensory Saltation" work of [10] to a 3×3 chair-mounted array. Eight possible directions are rendered to the Subject's back with two variations on thickness. Analysis showed responses were high above the 12.5% chance level, but recognition of thickness was negligible. A torso-mounted display in [7] provided aircraft pilots with orientation information. The authors performed simulated and in-flight tests. Within thirty minutes, Subjects correctly identified orientation by five degrees of pitch and roll.

In our original experiment [1], we addressed three parameters of a vibration pattern: position, direction, and profile. Each had one of two possible shapes: point and line. While Subjects in [1] identified each parameter at varying stages of the experiment, the focus of our newer study is position cuing. After observing mean error near zero at center of the array, then increase as stimuli moved away from the center, we postulated some systematic error was present in the data. Another form of systematic error is discussed in [11] and concerns the position identification of a glyph's profile. That is, the vibrotactile array rendered a line

Fig. 1. The vibrotactile array used in our experiment. Six rows of five pager motors are mounted on a project box containing a controller. The array is commanded via serial communication with a host computer.

with non-uniform intensity. Subjects indicated the pattern's center. It was found that responses tended to undershoot the target by a significant amount.

Envisioned for a collaborative visualization task, our device would convey supplementary information regarding other users and points of interest. Such a collaborative or guided exploration may require visual size to be scaled or correct answer reinforcement to be unavailable. These factors, along with a classification of Point Type, are examined for a position identification task. We then introduce a model of radial expansion and evaluate a proposed calibration method. This concept might then be extended to other haptic display devices, with a view to understanding the mechanisms behind this effect.

The remainder of this document proceeds as follows with a description of our haptic rendering system and the experimental methodology used in Section 2. Next, Section 3 presents the relevant statistical analysis and the calibration results. A discussion of the experimental results is then given in Section 4.

2 Experimental Methods

We conducted a repeated measures experiment to investigate the apparent trends in error and their relation to visual and haptic properties. Three Within-Groups variables were of interest: Subject (6 levels), Visual Size (3 levels), and Reinforcement (2 levels). We also considered one Between-Groups variable, Point Type (5 levels). We hypothesized that perceived position would be altered to the extent that some error would be systematic enough to be modeled for calibration.

2.1 Participants

We considered the six Subjects, S_1 to S_6, (all male) expert users for the purposes of this experiment. The use of experts reduced the effects of learning and better represented a regular user than a first time user. Although there were varying levels of prior experience with the device, each participated in previous experiment(s) with the palm-array and had training prior to data collection. Subjects

S_4 and S_5 were left-handed and the rest were right-handed. Subjects S_3 and S_6 were authors of this paper and had the most experience with our display device. The median age of subjects was 26 years, with a minimum age of 24 years and a maximum age of 37 years.

2.2 Materials

Subjects in our experiment were presented with tactile stimuli from the device shown in Figure 1. We chose a set of stimulus points that well-covered the array's motors. Also, we classified each stimulus point based on its position relative to nearby motors.

Apparatus The palm-sized vibrotactile array developed in [12] delivered stimuli during our experiment. The array consisted of six rows of five DC motors, each having a 14 mm diameter. We affixed nylon washers and foam pads above and below motors to isolate vibrations and allow a flexible-fit with the palm. A controller board housed within the project box provided serial communication with the host computer. To realize variations in intensity of vibrations, a pulse width modulation scheme was implemented on the host computer.

Software Treatment We defined a six by five grid with each cell centered on a motor. With centers of adjacent motors separated by 18 mm, this translated into grid cells measuring 18 mm x 18 mm. Two inherent limitations of our device were a low spatial resolution of motors and significant non-zero voltage needed for motor response. We approached the low resolution through unweighted area sampling, as in [13]. Gamma correction, another technique common in graphical rendering, addressed the motor response irregularities. Our extended gamma correction equation was

$$G(x;\alpha,\mu,\gamma) = \alpha\left[(1-\mu)x^{\frac{1}{\gamma}} + \mu\right], \tag{1}$$

where x is the input stimulus magnitude, α is a scaling factor, μ sets the lowest meaningful motor voltage, and γ is the standard gamma correction parameter. More information on this method is found in [13]. Through pilot studies with Subjects S_1 and S_2, we chose the parameters $\alpha = 0.8$, $\mu = 0.25$, and $\gamma = 1.925$ to ensure the different parts of the array had similar perceived intensities.

2.3 Design

For this experiment, we considered three independent variables: Point Type (Between-Groups), Visual Size (Within-Groups), and Reinforcement (Within-Groups). Subjects will also be treated as a Within-Groups variable in analysis. The four variants of a rendered point overlapping grid cells (as seen in Figure 2) identified the special cases for the Point Type. First, C1M denoted a point rendered on the center of one motor. The second and third special cases, E2H

and E2V, indicated a point between two horizontally or vertically adjacent motors, respectively. Specifically, E2H and E2V points were equidistant from two motor centers. The fourth case, termed E4N, was equidistant to four neighboring motors.

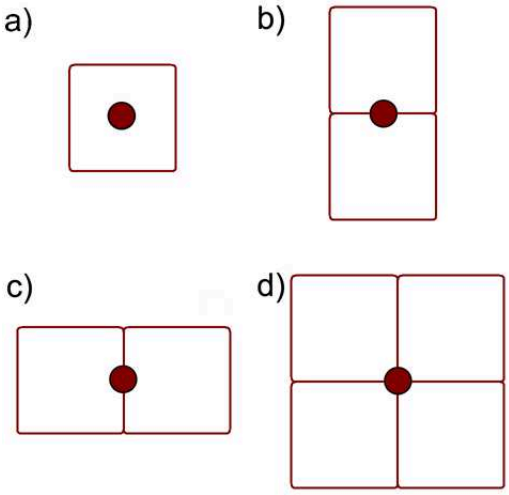

Fig. 2. Special Cases of Point Type. Squares represent motors and red circles represent stimuli. a) C1M: the center of one motor. b) E2V: equidistant between two vertically adjacent motors. c) E2H: equidistant between two horizontally adjacent motors. d) E4N: between four neighboring motors.

In total, there were 99 special case points, 30 C1Ms, 24 E2Hs, 25 E2Vs, and 20 E4Ns. We randomly generated 63 additional points spanning the region of interest. We called this set of points RAN. The experiment presented random permutations (randomization without replacement) of these 162 points to the Subjects in each session.

The next variable altered the rectangle in which Subjects marked answers on a graphical interface. The Visual Size had three levels: half-size (VSH), unit-size (VSU), and double-size (VSD). In the VSU level, the visual size of the rectangle in Figure 3 matched the array's size.

The presence or absence of reinforcement also varied, for the levels With Reinforcement (WR) and Without Reinforcement (WOR). During the WR level, the correct stimulus position appeared in the visual rectangle after the response was submitted.

2.4 Procedure

We conducted an open response experiment to investigate accuracy in locating vibrotactile position cues. Subjects wore liquid-filled, noise canceling headphones

Fig. 3. A screen capture of the data collection software. Stimulus (red) and response (green) marker circles were invariant of Visual Size. A sliding timer (top-right) was active during the stimulus, and a counter (bottom-right) informed Subjects of their progress during the trial.

with 29 dB attenuation of external sound. Each Subject completed six sessions, one per day on non-consecutive days. Each session consisted of a Demonstration, Training, and Testing Stage. The Demonstration Stage served to illustrate the form of stimuli and to allow comfortable placement of the Subject's palm. Subjects placed their left hand on the palm-array and felt a series of short point vibrations (each lasting two seconds). The array rendered five such points and the Subjects did *not* indicate position. During Training, Subjects marked the position of ten random points at the current day's experimental condition. The Testing Stage followed. We presented the entire point set consisting of 162 distinct stimulus points to the Subject. Subjects rested for at least 30 seconds at the mid-point of testing. Sessions generally lasted 30-40 minutes. Over the six days of testing, our group of six Subjects encountered $6 \times 6 = 36$ unique permutations of the point set. The organization of sessions is discussed below.

In the Training and Testing Stages, Subjects marked the position in a rectangle rendered on a computer monitor, as shown in Figure 3. The Training allowed Subjects to become accustomed to the current conditions. Responses were recorded with a custom software package and saved in an XML file.

Organization of Sessions The order of conditions (3 Visual Sizes $\times$ 2 Reinforcement Levels) was randomized but adhered to the following rules. On any given day, we presented all six condition combinations, one per Subject. A Subject's conditions consisted of visual levels in one order over the first three days, then the reverse order over days four through six. Reinforcement levels alternated between successive days of testing; half the Subjects started with reinforcement, half without. At least one day separated successive testing sessions of a Subject.

3 Results and Discussion

3.1 Error Magnitude Metric

We performed an ANOVA for Repeated Measures over the 36 experimental conditions (6 Subjects × 3 Visual Sizes × 2 Reinforcement Levels) and the dependent variable error magnitude. The experiment also included a Between-Groups variable of Point Type.

We report significant effects for each Within-Groups factor. Most notably, the Subjects exhibited significant differences ($F(4,5) = 92.57, p < 0.001$), as did the Visual Sizes ($F(4,2) = 8.72, p < 0.001$). WR had less overall error than WOR ($F(4,1) = 8.43, p < 0.005$). Additionally, the analysis detected interactions between Visual Size and Reinforcement ($F(4,2) = 3.51, p < 0.05$).

Post-Hoc tests with Bonferroni corrections gave us comparisons of Subjects and Visual Sizes. After aggregating results, we found that S_5 performed the best, having significantly less error than all but S_1, who was a close second. Counter to this, S_6 performed worse than all other Subjects. Interestingly, S_6 had substantially more experience than all but S_3, and neither S_3 nor S_6 was the best performing user. However, S_3 did perform more consistently over different visual sizes and reinforcements than any other user.

For Visual Size, tests showed VSH to produce less error than both VSU and VSD. The interaction between Visual Size and Reinforcement is evident in the last pairing of Figure 4. Recall that VSH's error magnitude was significantly less than VSU and VSD. As Visual Size increased, it was initially the dominant effect. Then, noting that pooled VSU and VSD error magnitudes were roughly similar, Reinforcement became more of an influence at the level VSD. This observation gives credence to our initial hypothesis that both Visual Size and Reinforcement affect accuracy.

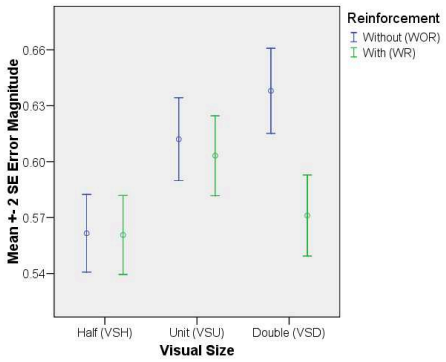

Fig. 4. Error magnitude against Visual Size and Reinforcement. The large change between the last pair of error bars illustrates the interaction between Visual Size and Reinforcement.

For the Between-Groups factor Point Type, Post-Hoc tests indicated a lower error magnitude at C1M points compared to RAN and E2H. E2V was a borderline result, with a near significant p-value below 0.06. This trend was consistent for all between-motor points, if not at a significant level. Figure 5 shows the near significant result of E2V as well as the similarities between other such stimuli. Further inspection of separate X and Y error components also suggests that error is smaller at motor centers than between motors. E2V was the most notable example of this.

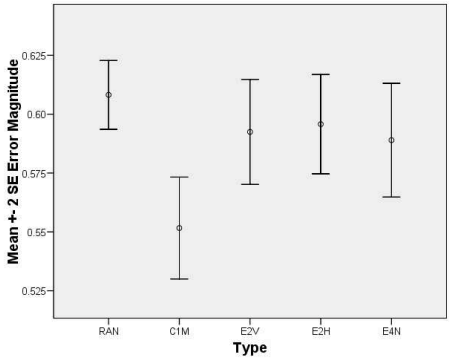

Fig. 5. Error magnitude by point type. The between-motor types RAN, E2H, E2V, and E4N were consistently higher than C1M.

Upon further examination of error vectors centered on stimulus points, see Figure 6, there appeared to be a trend of radial expansion, described next. As the stimulus' distance from the array's center increased, error vectors seemed to lengthen, then contract. Also, the orientation of error vectors tended to point roughly away from the array center. To measure this effect, we considered the signed metric of radial error, defined to be $e_r = \hat{s} \cdot \mathbf{e}$, where $\hat{s}$ is the normalized radius from array center and $\mathbf{e} = R - S$, as in Figure 7.

3.2 Radial Error Metric

For the purposes of analyzing radial error, we transformed stimulus and response points into a canonical coordinate system such that the array center was the origin and $y' = \frac{4}{5}y$. This scaling of y made all stimulus and response radii of a given length extend equally on the array. We performed another ANOVA over the metric radial error. Post Hoc tests showed VSH to cause significantly less error than VSU and VSD ($F(4, 2) = 33.136, p < 0.001$). In Figure 8, however, we saw some measure of radial expansion for all three levels of the variable. VSU had a more pronounced increase, and a higher peak, than the other levels. That said, Subjects were more prone to systematic error when not given reinforcement for VSD. This can be deduced from the significant interaction between Visual

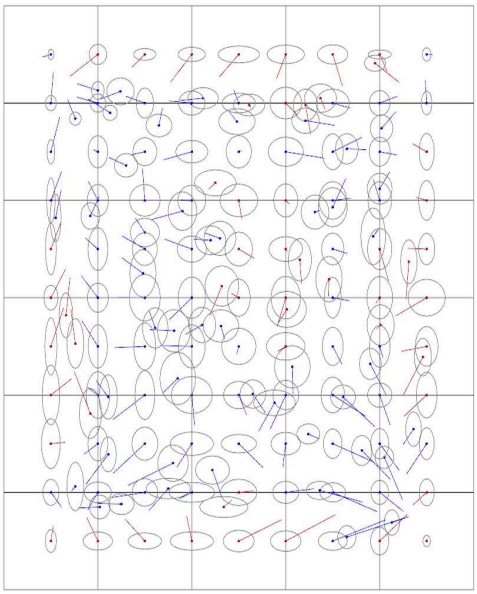

Fig. 6. Error vectors rendered at stimulus points. Ellipses represent standard error in both dimensions. Error vectors represent mean error for the point. Blue error vectors represent positive radial error, red represent negative radial error. Shown is the condition WR.

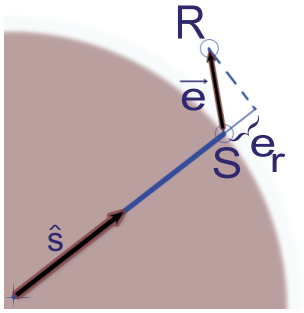

Fig. 7. Radial error derivation with the stimulus point S and associated response R. The point S defines a vector **s** from the origin to S, R defines the error vector **e** from S to R. Radial error e_r is the directed magnitude of **e** projected onto the normalized $\hat{s}$.

Size and Reinforcement over the metric of radial error ($F(4, 2) = 5.577, p < 0.05$) and the doubling of mean radial error from VSD-WR to VSD-WOR.

This radial error metric e_r gave us the directed magnitude of **e** projected onto $\hat{s}$, or more concisely, how far from the stimulus' radius the Subject responded. Plotting $\|\mathbf{s}\|$ against e_r and applying a local linear regression (smoother), we saw curves characteristic of our previous observations, e.g. Figure 8. Regression estimates started near zero at zero radius (array center) and began to rise. They

then reached a clear global maximum and decreased. This suggested a quadratic relationship between stimulus radius and radial error as a preliminary model to test the feasibility of calibrating for the effect.

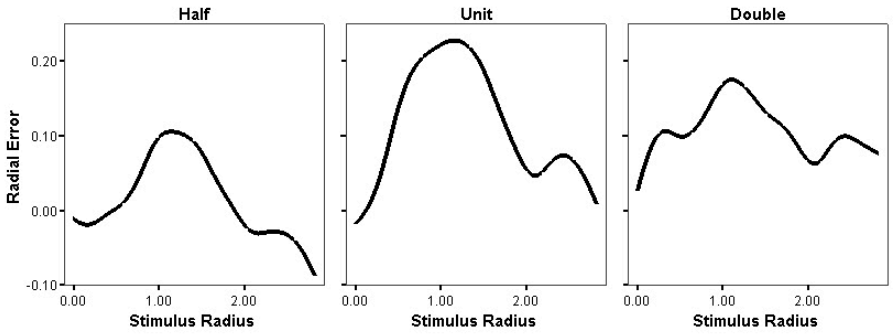

Fig. 8. Radial Error Smoothers by Visual Size. Each case contains some unimodal behavior. The Unit Visual Size (VSU) experienced the highest peak of radial error. VSH contained significantly less radial error than both VSU and VSD.

From the pairs $(\|\mathbf{s}\|, \|\mathbf{s}\| + e_r)$, we fitted a quadratic function f[1] via Singular Value Decomposition to a random half of the data. Then, f^{-1} estimated a stimulus radius $\|\mathbf{s}\|'$ that would be applied during calibration. A 2-fold cross validation (holdout method) compared the error before and after our calibration estimate as $(\|\mathbf{s}\| + e_r) - \|\mathbf{s}\|$ and $(\|\mathbf{s}\| + e_r) - \|\mathbf{s}\|'$.

Two assumptions were made concerning the inversion. The first constrained the endpoints of the model function: $f(0) \approx f(L) \approx 0$, where L was the maximum radius of the array. The second required the linear coefficient to $b < 2$. When these requirements were met, however, we were able to adjust the stimulus radius in an estimate of a calibration procedure. After calibration, we detected lower error for Subjects S_2, S_3, and S_5 ($F(1, 658) = 125.64, 393.92, 4.62; p < 0.05$) and for all Subjects pooled ($F(1, 3958) = 213.28, p < 0.001$). An increase in mean absolute error occurred for both S_1 and S_6, only the latter of which was significant ($F(1, 658) = 56.65, p < 0.05$). The calibration routine was not applicable to S_4's stimuli given the above constraints. Accordingly, we reported no results for this Subject.

To better visualize the effect of radial expansion over the levels of Visual Size, we constructed a warped stimulus grid from mean error vectors. As seen in Figure 9, we computed the mean response for each response point, excluding the case RAN. In each level of Visual Size, radial expansion was present to some extent. Expansion began near the center of the array, characterized by the relative area of warped to non-warped cells. The expansion also caused neighboring cells to shift from the original cell centers. A contraction near the grid edges countered

[1] If the fit over $(\|\mathbf{s}\|, e_r)$ gives $f(x) = a + bx + cx^2$, then our fit over $(\|\mathbf{s}\|, \|\mathbf{s}\| + e_r)$ gives $f'(x) = a + bx + cx^2 + x = a + (b + 1)x + cx^2$.

the interior expansion. Mean error vectors placed edge point responses closer to the array center. These general trends reinforced our understanding of radial expansion and illustrated its relationship to Visual Size.

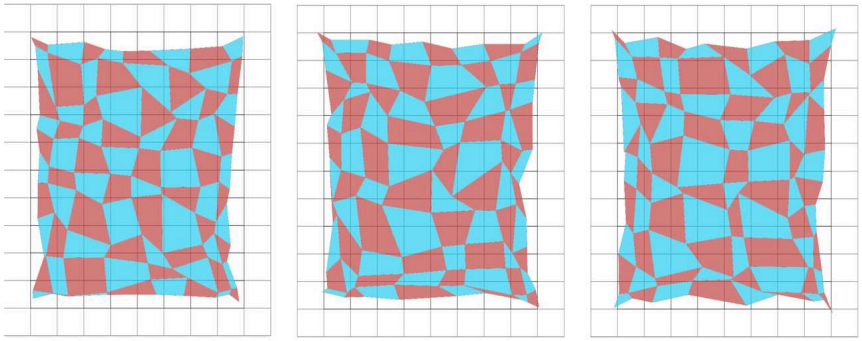

Fig. 9. Warped grid representing mean stimulus-response mapping for each level of Visual Size. Left is Half size (VSH), middle is Unit size (VSU), and right is Double size (VSD). Each colored quadrilaeral is mapped from a cell in the underlying grid. Only Point Types C1M, E2H, E2V, and E4N.

4 Conclusion

The statistical significance from our experimental conditions shows their importance in improving accuracy of tactile displays. When users are presented with such stimuli, care must be taken to account for different types of systematic error. The relevant factors should be identified and their effects mediated. Herein, we demonstrated such factors for positional cuing.

Our observations confirmed the research hypothesis for each condition of the experiment. Visual Size had the most effect on error magnitude for VSH and VSU, then Reinforcement had a significant effect. We observed identical results for the metric radial error and confirmed the systematic error thought to be present in a previous study. By modeling the radial error with a quadratic fit, we were able to give some insight as to the source of the error and possibly provide a calibration for it.

To varying extents, each Subject exhibited a discernable effect of radial expansion. The significant differences among users indicated another consideration for our model. Several users were clearly distinguishable from one another and others less so. This made the choice of pooled or per-user calibration difficult. The simplest effective model was a pooled, quadratic fit over all data. A significant decrease in error was achieved here. A model better fit to the data may be a quadratic regression spline with several knot points [14].

The trends above also suggested that radius alone does not fully model radial expansion. A natural choice for a second model variable would be angular

measure. This would make our model a surface, multifaceted and having multiple inverses. The warped stimulus grid from Figure 9 could serve as yet another alternative model. Choices for resolution, interpolation, and regression would impact the effectiveness of such a strategy.

The effects of radial expansion and the possibility of calibrating for it were evaluated. The context, exploration of some dataset with vibrotactile position cues, informed our choice of design variables. From these concepts, extension to other tactile display devices is possible. Further studies should examine the role of Visual Size in calibration and how Visual Sizes between unit and double spread with respect to Reinforcement.

References

1. Baiyya, V.B.: Design and Evaluation of a Haptic Glyph System for 2D Vibrotactile Arrays. Master's thesis, University of Louisiana at Lafayette (2007)
2. Pietrzak, T., Pecci, I., Martin, B.: Static and Dynamic Tactile Directional Cues Experiments with VTPlayer Mouse. In: Proceedings of the Eurohaptics International conference EuroHaptics 2006. pp. 63–68, Paris, France (2006)
3. Chen, H., Santos, J., Graves, M., Kim, K., Tan, H.: Tactor Localization at the Wrist. pp. 209–218, Madrid, Spain (2008)
4. Cholewiak, R.W., Brill, C.J., Schwab, A.: Vibrotactile Localization on the Abdomen: Effects of Place and Space. Perception and Psychophysics, pp. 970–987 (2004)
5. Cholewiak, R.W., Collins, A.A.: Vibrotactile Localization on the Arm: Effects of Place, Space and Age. Perception and Psychophysics 65, pp. 1058–1077 (2003)
6. Cholewiak, S., Tan, H., Ebert, D.: Haptic Identification of Stiffness and Force Magnitude. Haptic Interfaces for Virtual Environment and Teleoperator Systems, pp. 87–91 (2008)
7. Rupert, A.H.: An Instrumentation Solution for Reducing Spatial Disorientation Mishaps. IEEE Eng Med Biol 19, pp. 71–81 (2000)
8. Tan, H., Lim, A., Traylor, R.: A Psychophysical Study of Sensory Saltation with an Open Response Paradigm. In: Proceedings of the Ninth (9th) International Symposium on Haptic Interfaces for Virtual. pp. 1109–1115 Volume 69., Orlando, FL (2000)
9. van Erp, J.B.F., van Veen, H.A.H.C., Jansen, C., Dobbins, T.: Waypoint Navigation with a Vibrotactile Waist Belt. ACM Trans. Appl. Percept. 2, pp. 106–117 (2005)
10. Tan, H.Z., Pentland, A.: Tactual Displays for Wearable Computing. Personal Technologies 1, pp. 225–230 (1997)
11. Borst, C.W., Baiyya, V.B.: A 2D Haptic Glyph Method for Tactile Arrays: Design and Evaluation, to appear in Worldhaptics 2009. (2009)
12. Borst, C.W., Cavanaugh, C.D.: Touchpad-Driven Haptic Communication Using a Palm- Sized Vibrotactile Array with an Open-Hardware Controller Design. In: Proceedings of the EuroHaptics 2004 Conference. pp. 344–347 (2004)
13. Borst, C.W., Asutay, A.V.: Bi-Level and Anti-Aliased Rendering Methods for a Low-Resolution 2D Vibrotactile Array. In: WHC '05: Proceedings of the First Joint Eurohaptics Conference and Symposium on Haptic Interfaces for Virtual Environment and Teleoperator Systems. pp. 329–335, Washington, DC, USA, IEEE Computer Society (2005)

14. Ruppert, D., Wand, M., Carroll, R.: Semiparametric Regression. Cambridge University Press, United Kingdom (2003)